Electronic Supplementary Material (ESI) for Polymer Chemistry.

Supplementary information

The role of tertiary amines as internal catalysts for disulfide exchange in covalent adaptable networks

Kanta Yamawake, Mikihiro Hayashi

Department of Life Science and Applied Chemistry, Graduate School of Engineering,
Nagoya Institute of Technology, Gokiso-cho, Showa-ku Nagoya 466-8555, Japan

1. Materials

Butyl acrylate (BA), 2-(dimethylamino)ethyl acrylate (DMAEA), (3,4-epoxycyclohexyl)methyl acrylate (ECHMA), 4-hydroxybutyl acrylate (HBA), phenyl acrylate, triethylamine (TEA), 2,2′-dithiodibenzoic acid, 2,2′-biphenyldicarboxylic acid, 3,3′-dithiodipropionic acid, and *N*,*N*,*N*′,*N*′-tetramethyl-1,6-diaminohexane were purchased from TCI. 2-Cyano-2-propyl dodecyl trithiocarbonate was purchased from Aldrich. Azobisisobutyronitrile (AIBN) was purchased from FUJIFILM Wako Pure Chemical Corporation. Propylamine (PA) was purchased from Nacalai tesque. BA, DMAEA, ECHMA and HBA were purified by passing them through alumina prior to use. Other chemicals and organic solvents were used as recieved.

2. Analytical methods

Molecular chracterization:

Number average molecular weight (M_n) and dispersity index ($Đ$) were investigated by size exclusion chromatography (SEC). For the measurements, the set-up used was JASCO PU4185 pump system, equipped with JASCO RI-4035 differential refractometer and JASCO CO-2065 Plus Intelligent Column Oven [eluent, tetrahydrofuran (THF), flow rate = 0.35 mL/min, temperature = 40 °C; Tosoh Inc.]. Poly(methyl methacrylate)s were used as standards. The syntheses of the terpolymers were confirmed by ^{1}H-NMR in $CDCl_3$ or DMSO-d_6 (depending on the solubility) with using a Bruker Analytik DPX400 spectrometer (400 MHz), which was also used to estimate the degree of polymerization. The cleavage of the RAFT residue in the terpolymer was confirmed via UV-vis spectroscopy using an F-2700 (Hitachi High-Tech) in the solution state.

Fourier transform infrared spectroscopy (FT-IR):

The cross-linking reaction was confirmed by FT-IR spectroscopy. The measurements were conducted at 25 °C using an FT/IR 430 spectrometer with an attenuated total reflectance (ATR) attachment (JASCO Co.).

Swelling test:

Swelling tests were conducted to assess the swelling ratio (R_s). The disc-shaped specimens with 8 mm diameter and 0.5 mm thickness were immersed in the solvent (THF). After one day immersion, R_s was estimated, according to $R_S = \left(\frac{d_s}{d_i}\right)^3 \times 100$, where d_i and d_s are the diameter of initial and swollen samples, respectively. The gel fraction (ϕ_{gel}) was also estimated by the swelling test. The swollen sample was completely dried by vacuum, and the dried mass (m_d) was compared with the initial mass (m_i). The ϕ_{gel} was estimated by the relationship, $\phi_{gel} = \frac{m_d}{m_i} \times 100$.

Thermal properties:

Glass transition temperatures (T_gs) were measured by differential scanning calorimetry (DSC) with using DSC7020 (HITACHI). The data was taken from the second heating from -70 to 100 °C at a constant temperature ramp rate of 10 °C/min. Thermogravimetric analysis (TGA) was performed to investigate the thermal decomposition temperature with using TG/DTA7300 (HITACHI). The temperature ramp rate was set to 10 °C/min. All the above thermal investigations were performed for approximately 10 mg samples under N_2 gas flow.

Temperature-sweep rheology:

Uniaxial rheology with a temperature-sweep mode was performed using DMS6100 (HITACHI High-Tech). A strip-shaped sample with 0.5 mm in thickness, 4 mm in width, and 20 mm in length was used for the measurement. The frequency was fixed to 1 Hz, and the constant strain of 0.1 % was applied during the measurement. The temperature was increased from -50 °C to 200 °C with a rate of 5 °C/min. All the measurements were performed under N_2 gas flow.

Temperature-ramp creep:

The softening temperature was investigated by temperature-ramp creep test using TMA7100 (HITACHI High-Tech). A rectangular-shaped sample with 20 mm length, 4 mm width, and 0.5 mm thickness, was used. To estimate the softening temperature at which the bond exchange was activated, the sample length change was detected with increasing temperatures at 5 °C/min under a very small constant tension (25 kPa << sample modulus) to avoid sample bending. All the measurements were performed under N_2 gas flow.

Stress relaxation:

Stress relaxation dynamics was measured with an application of 3% strain, using a shear-type rheometer (MCR302, TA Anton paar) and 8 mm parallel plates. The disc-shaped samples with 8 mm diameter and 0.5 mm thickness were prepared using a cutting die. The tests were carried out at various temperatures, and the samples were kept for 20 min at each target temperature for thermal equilibration before the measurements. All the measurements were performed under N_2 gas flow.

ESR:

ESR spectra were obtained with JEOL X-band (ca. 9 GHz) FA200 spectrometers with 100 kHz field modulation at a microwave power of 0.4 mW to avoid power saturation and the modulation width of 0.1 mT. The magnetic field width, sweep time, and time constant were typically 15 mT, 120 s, and 0.1 s, respectively. Samples were encapsulated into 5 mm o.d. quartz tubes and sealed under a vacuum. Each measurement was started after the sample was equilibrated at target temperatures (160 or 120 °C) for 5 min. The magnetic field and *g*-value were calibrated with Mn^{2+} in MgO.

3. Synthesis protocols

3-1. Synthesis of P-N

P-N was synthesized according to Scheme S1.

Scheme S1. Synthesis of P-N

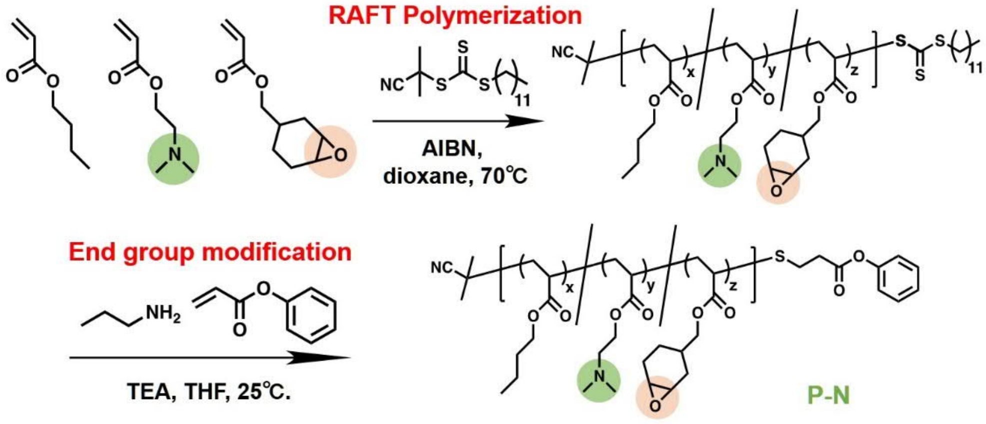

To obtain the target terpolymer, copolymerization of butyl acrylate (BA), 2-(dimethylamino)ethyl acrylate (DMAEA), (3,4-epoxycyclohexyl)methyl acrylate (ECHMA) was first carried out via RAFT polymerization. The mixture solution of BA, DMAEA, ECHMA, chain transfer agent (CTA), and radical initiator was prepared in 1,4-dioxane using a 50 mL flask. 2-Cyano-2-propyl dodecyl trithiocarbonate and azobisisobutyronitrile (AIBN) was used as the CTA and radical initiator, respectively. The feed ratio of BA : DMAEA : ECHMA was set to 6: 1: 1, and the monomer weight concentration was 50%. The feed mole ratio of monomers ($[M_{total}]$), CTA ([CTA]), and AIBN ([AIBN]), was set to $[M_{total}]$: [CTA] : [AIBN] = 400: 1: 0.08. After N_2 bubbling for 15 min, the copolymerization was conducted at 70 °C for 4 h. The obtained terpolymer was purified by reprecipitation using THF as a good solvent and hexane as a poor solvent. The obtained terpolymer was coded as P-N.

The RAFT residue in the end group was then modified to avoid dimerization reaction during physical property investigation at high temperatures. The polymer was dissolved in THF, and then propylamine (PA), phenyl acrylate (PhA), and triethylamine (TEA) were added and homogenized. The feed mole ratio of P-N ([P-N]), PA ([PA]), PhA ([PhA]), and TEA ([TEA]) was set to [P-N]: [PA]: [PhA]: [TEA] = 1: 30: 10: 0.33. The weight concentration of P-N was 20% in the THF solution. The reaction was conducted at 25 °C for 24 h. In this reaction, aminolysis and Michael addition reaction simultaneously progressed. After the reaction, purification was conducted by reprecipitation using THF as a good solvent and hexane as a poor solvent. The cleavage of RAFT residue (i.e., trithiocarbonate group) in the end group was confirmed by UV-vis spectrum.

3-2. Synthesis of P-OH

As a control sample, a terpolymer without tertiary amines was synthesized. In this case, DMAEA was replaced with 4-hydroxybutyl acrylate (HBA) in the above synthesis scheme. Concretely, copolymerization of BA, HBA, and ECHMA was carried out via RAFT polymerization. The mixture solution of BA, HBA, ECHMA, chain transfer agent (CTA), and radical initiator was prepared in 1,4-dioxane using a 50 mL flask. 2-Cyano-2-propyl dodecyl trithiocarbonate and AIBN was used as the CTA and radical initiator, respectively. The feed ratio of BA: HBA: ECHMA was set to 4.5: 2.5: 1, and the monomer weight concentration was 50%. The feed mole ratio of monomers ([M_{total}]), CTA ([CTA]), and AIBN ([AIBN]), was set to [M_{total}]: [CTA]: [AIBN] = 400: 1: 0.08. After N_2 bubbling for 15 min, the copolymerization was conducted at 70 °C for 1.5 h. The obtained copolymer was purified by reprecipitation using THF as a good solvent and a mixture solvent of water/methanol (water/methanol = 1/1 vol.) as a poor solvent. The obtained copolymer was coded as P-OH.

The RAFT residue in the end group was then modified to avoid dimerization reaction during physical property investigation at high temperatures. The reaction condition was the same as that for the case of P-N. The cleavage of RAFT residue (i.e., trithiocarbonate group) in the end group was confirmed by UV-vis spectrum.

4. Blend and cross-linking reaction

P-N was blended with a diacid cross-linker containing a disulfide bond (2,2’-dithiodibenzoic acid) via solution casting. The polymer and cross-linker were individually dissolved in THF where the feed mole ratio was epoxy: COOH = 1: 1, and the solutions were mixed in a Teflon-made mold. The solvent was evaporated by heating on a heating plate at 40 °C for 24 h, followed by vacuum drying. For cross-linking, the bulk mixture sample was heated at 100 °C for 48 h, resulting in a stable elastic film. The control sample using P-OH was prepared with the same way.

5. Preliminary experiment using small molecules

As a preliminary experiment, we checked the role of tertiary amines for activation of disulfide exchange using small molecules. 3,3′-dithiodipropionic acid (DPA) and 2,2′-dithiodibenzoic acid (DBA) (see Scheme S2) were kept stirring in the presence or absence of a tertiary amine molecule, *N*,*N*,*N′*,*N′*-tetramethyl-1,6-diaminohexane, at 130 °C for 70 min in the solution state using a mixture solvent of DMSO/1,4-dioxane. The solvents were then evaporated, and the residue was measured for ^{1}H-NMR (DMSO-d_6). In the absence of the tertiary amine molecules (Figure S1), the signals from starting DBA remained the same, and new signals from exchanged product was negligible. On the other hand, new signals clearly appeared for the system in the presence of the tertiary amine molecules (Figure S2), and these new signals are assgined to the molecule generated from exchange reaction of DPA and DBA. These results indicate that tertiary amine played an important role for activation of disulfide exchange.

Scheme S2. Model reaction of DBA and DPA for preliminary experiment

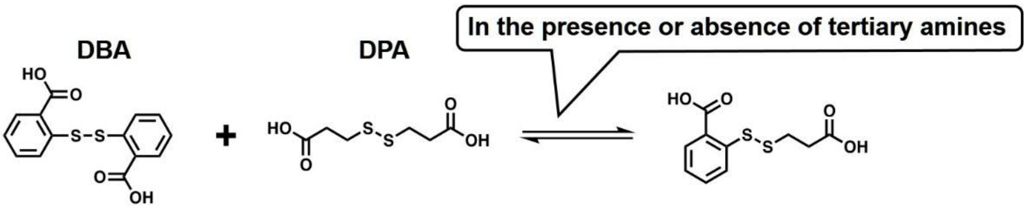

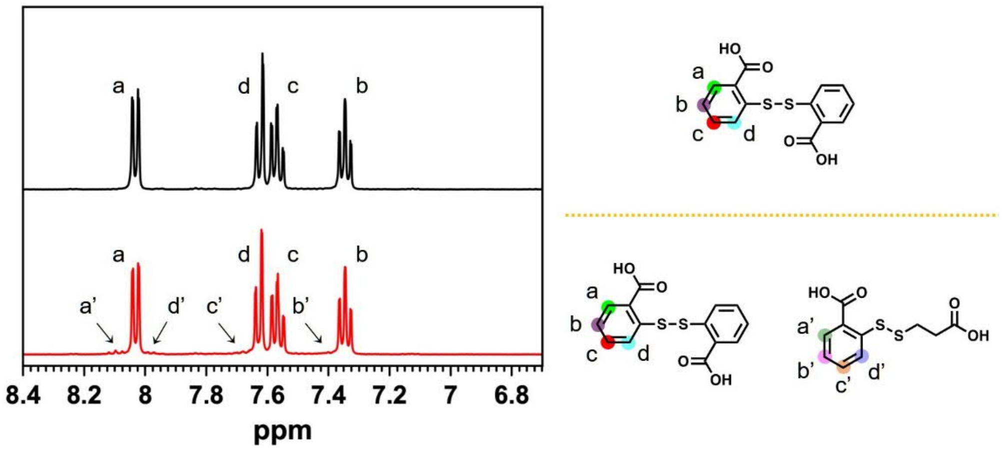

Figure S1. ^{1}H-NMR spectra for starting DBA (top) and the residue after stirring in the absence of tertiary amines (bottom). Hx with alphabet (x) in the spectra corresponds to the protons with the same alphabet in the chemical structures.

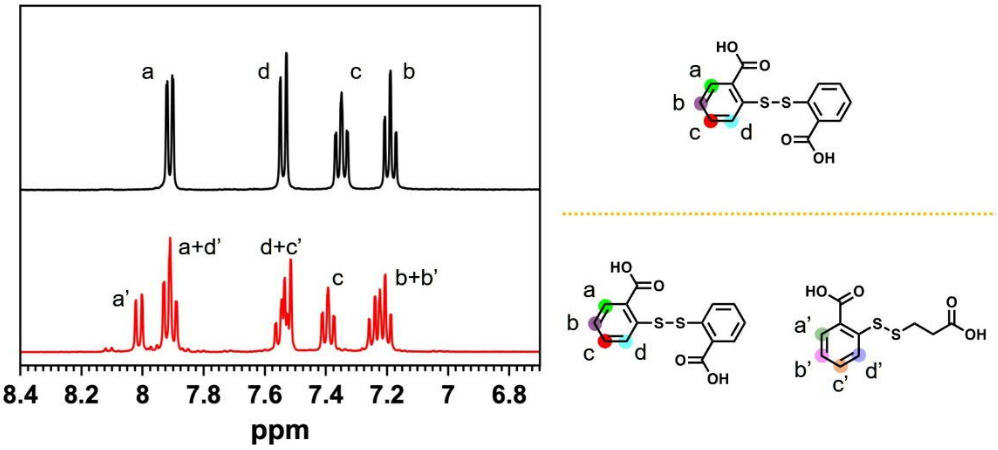

Figure S2. ^{1}H-NMR spectra for starting DBA (top) and the residue after stirring in the presence of tertiary amines (bottom). Hx with alphabet (x) in the spectra corresponds to the protons with the same alphabet in the chemical structures. Note that the signal position was slightly different from that in Figure S1, which is due to the presence of amines that should have some interaction with COOH group.

6. ^{1}H-NMR spectra

Syntheses of P-N and P-OH were confirmed by ^{1}H-NMR (Figure S3 and S4). In the Figures, Hx with alphabet (x) in the spectra corresponds to the protons with the same alphabet in the chemical structures. In the spectrum of P-N (Figure S3), the integral ratio of H_c, H_e, and H_m was used for the estimation of the unit mole ratio of BA, DMAEA, and ECHMA units. In the spectrum of P-OH (Figure S4), the integral ratio of H_c, H_o, H_m, and H_n was used for the estimation of the unit mole ratio of BA, HBA, and ECHMA units.

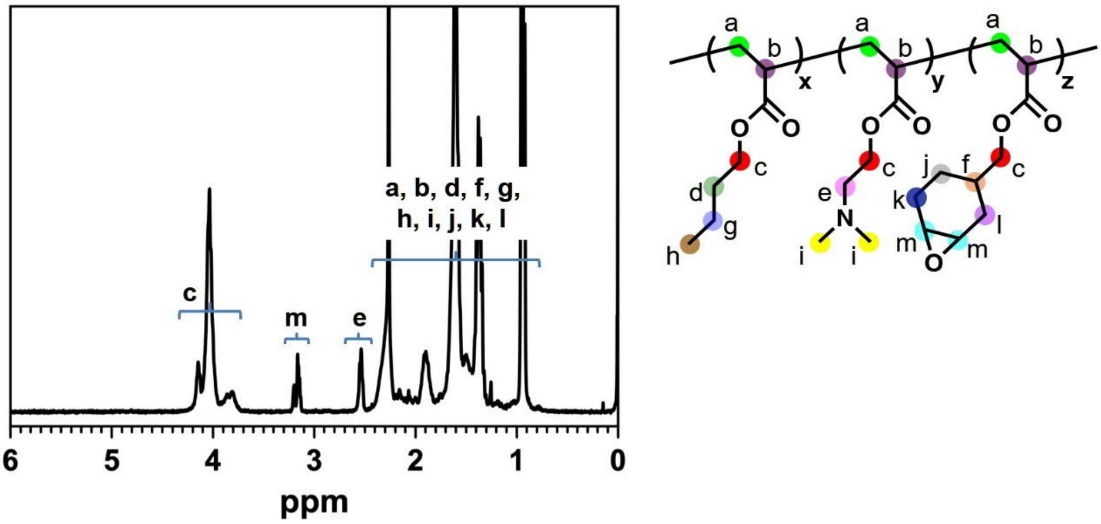

Figure S3. ^{1}H-NMR spectrum of P-N in $CDCl_3$.

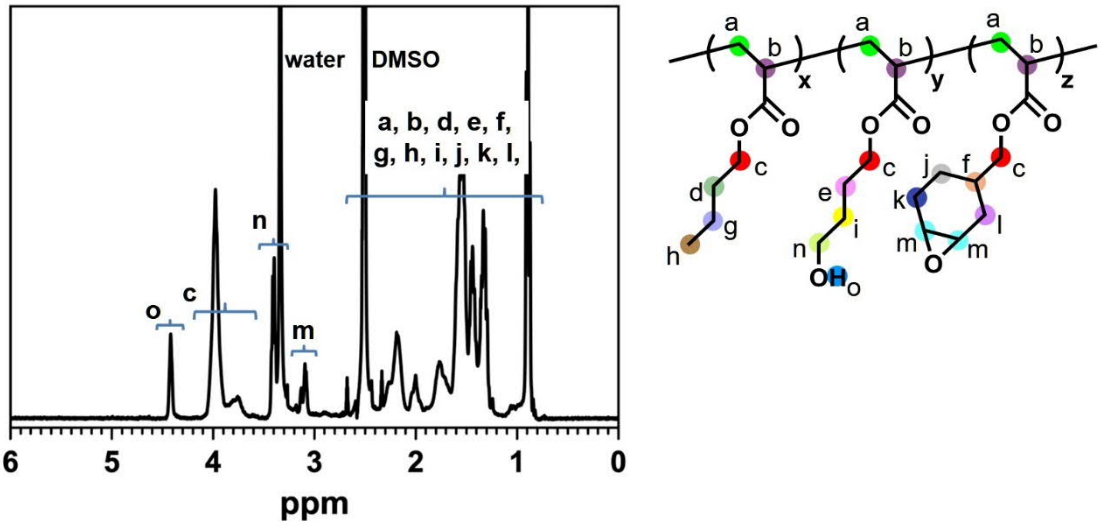

Figure S4. ^{1}H-NMR spectrum of P-OH in DMSO-d_6.

7. SEC curves

Figure S5 summarizes the SEC curves for P-N and P-OH, in which the data of the samples before and after cleavage of the end RAFT residue are shown.

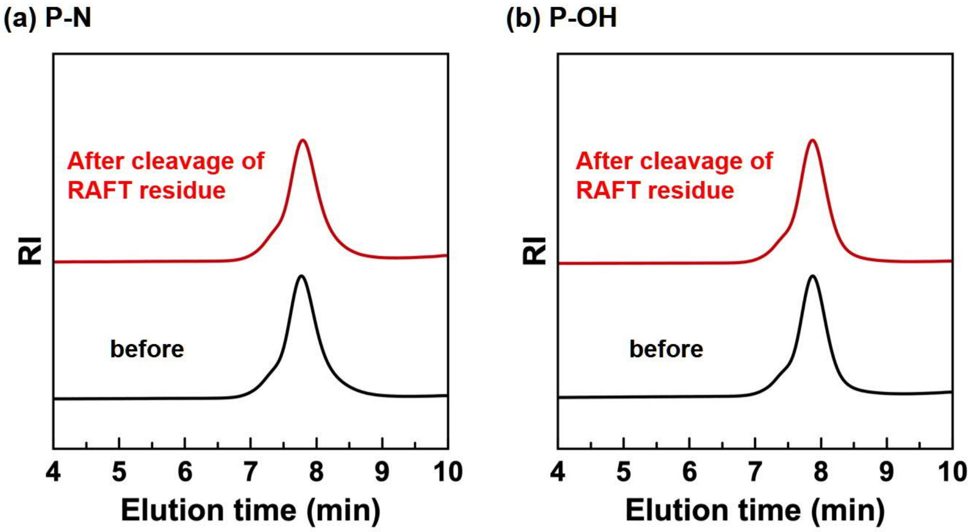

Figure S5. SEC curves for P-N and P-OH before and after cleavage of the end RAFT residue.

8. UV-vis spectra

Figure S6 summarizes the UV-vis spectra for P-N and P-OH before and after cleavage of the RAFT residue.

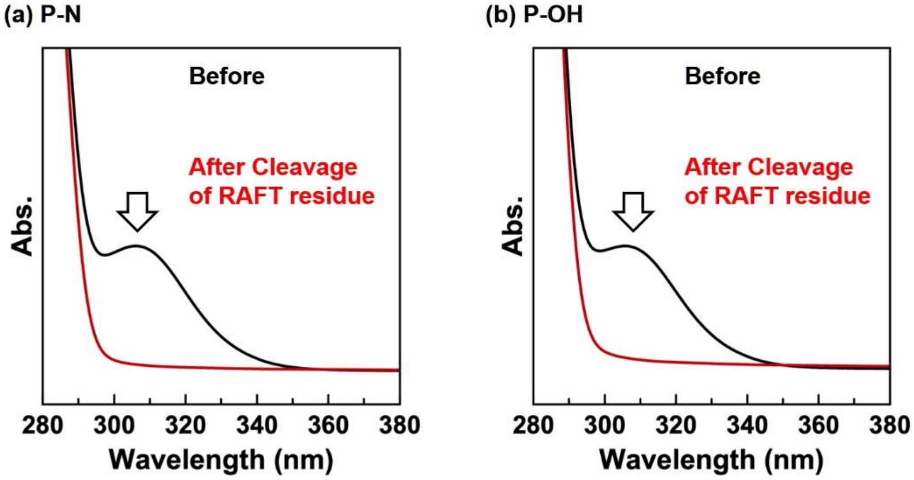

Figure S6. UV-vis spectra for P-N and P-OH before and after cleavage of the RAFT residue. The arrows indicate the characteristic absorption signal from the trithiocarbonate end group.

9. FT-IR spectra

Figure S7 represents the FT-IR spectra before and after cross-linking reaction.

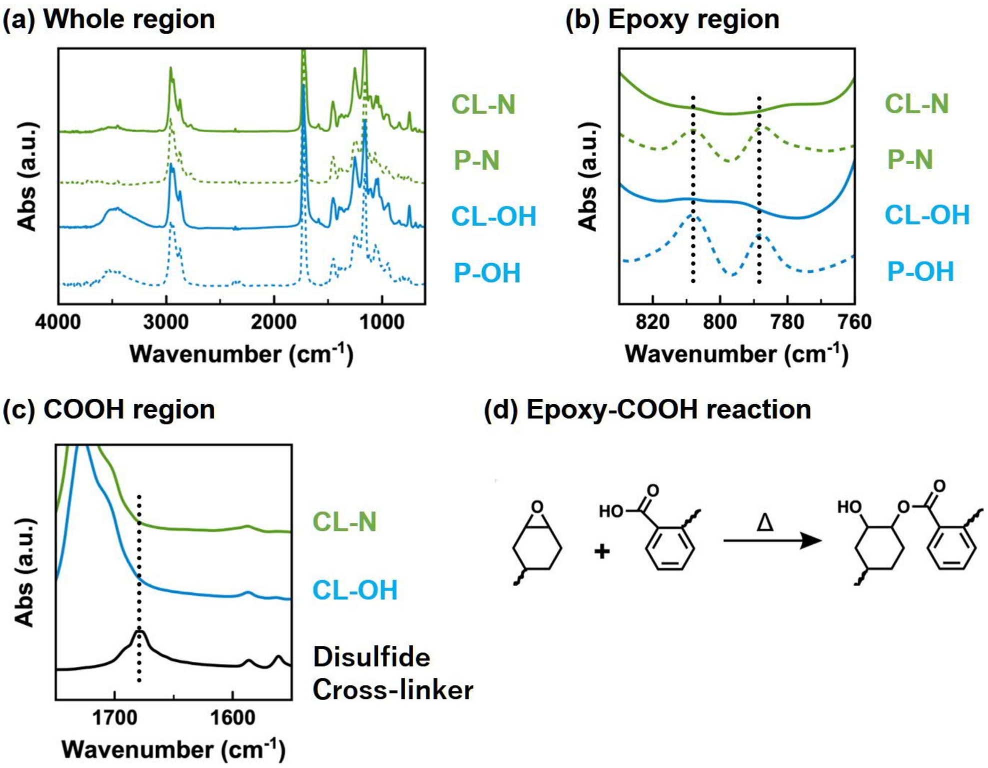

Figure S7. FT-IR spectra for the precuror polymers and cross-linked samples at (a) whole region, (b) epoxy region, and (c) COOH region. The dotted lines in (b) and (c) indicate the signals from epoxy and the signal from COOH group, respectively, according to the literature (refs #56 and 57 in the main text). Schematic of the reaction between COOH and epoxy is shown in (d).

10. DSC data

Figure S8 summarizes DSC data for the precursor polymers (P-N and P-OH) and cross-linked samples (CL-N and CL-OH).

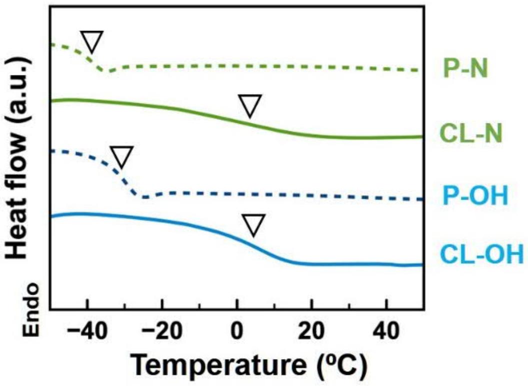

Figure S8. DSC thermograms for the samples before and after cross-linking reaction. The data were obtained in the second heating. The inverse triangles represent T_g.

11. TGA thermograms

Figure S9 summarizes TGA thermograms for the cross-linked samples.

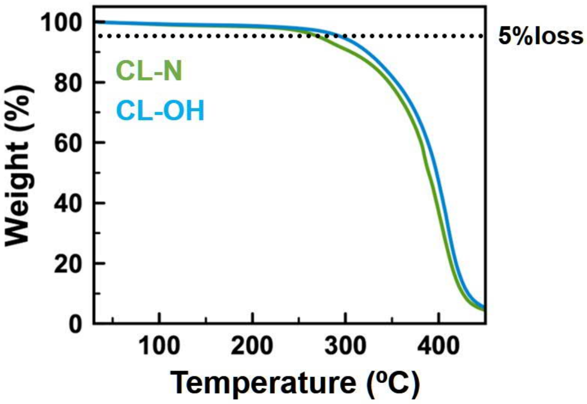

Figure S9. TGA thermograms for the cross-linked samples.

12. Relaxation data for the sample without disulfide

As a control sample, a cross-linked sample without disulfide units was prepared. The precursor polymer was P-N, and the cross-linker molecule, 2,2′-biphenyldicarboxylic acid (see the chemical structure in Figure S10), was used. Stress relaxation curve at 160 ºC is shown in Figure S10, where the relaxation was negligible due to the absence of disulfide bond.

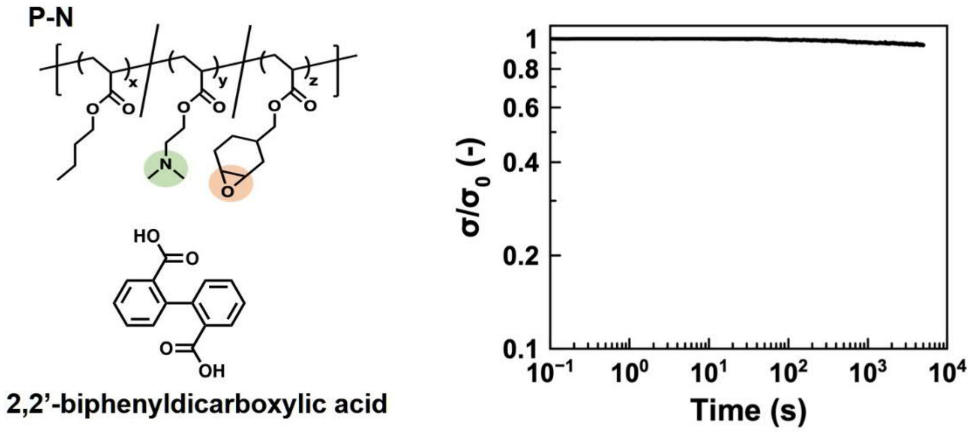

Figure S10. Stress relaxation data at 160 ºC for the control sample without disulfide bonds.

13. Relaxation data for CL-OH in the presence of external amine catalysts

We performed a stress relaxation test at 160 ºC for CL-OH in the presence of external amine catalysts, *N,N,N′,N′*-tetramethyl-1,6-diaminohexane. The sample was prepared by cross-linking of P-OH with an addition of the amine catalysts via solution casting. The mole ratio of amines to disulfide bonds was the same as that in CL-N for fair comparison. The relaxation rate was faster for this sample with external amine catalysts than CL-N, which may be due to the larger mobility of the amine molecules.

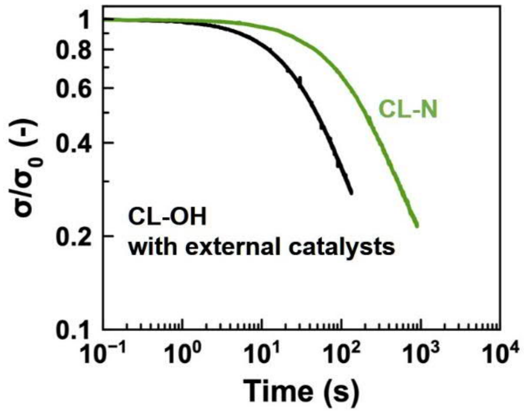

Figure S11. Stress relaxation curve for CL-OH with external amine catalysts, where the data for CL-N is also shown for comparison. In the Y-axis, the stress (σ) was normalized by the initial stress (σ_0). The data were taken at 160 ºC.

14. Temperature dependence of the stress relaxation for CL-N and CL-OH

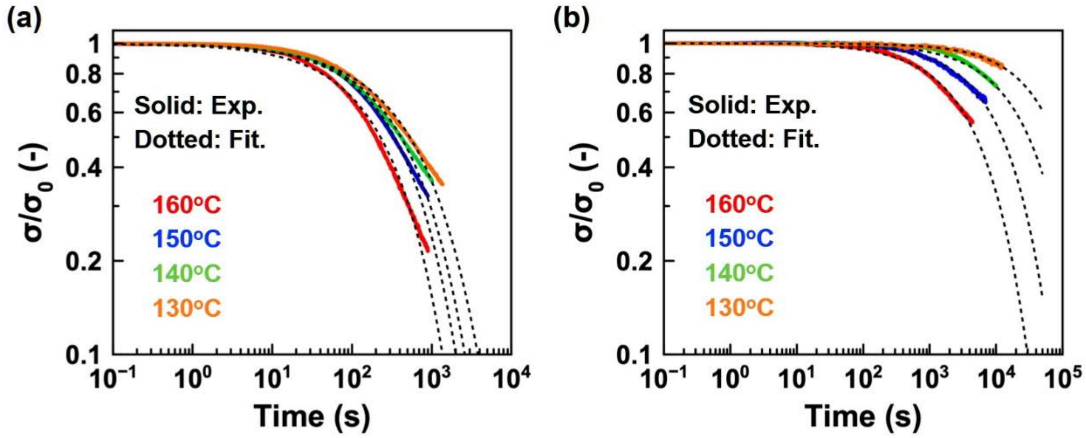

Figure S12. Stress relaxation curves for (a) CL-N and (b) CL-OH at various temperatures. In the Y-axis, the stress (σ) was normalized by the initial stress (σ_0). The dotted curves indicate the fitting curves based on the KWW function (see main text).

Table S1. Summary of fitting parameters and $<\tau>$ for CL-N

Temperature (°C)	τ (s)^{a}	β (-)^{a}	$<\tau>$ (s)
130	970	0.61	1430
140	725	0.65	990
150	590	0.68	770
160	385	0.63	550

a) see the explanation of the fitting parameters in the main text.

Table S2. Summary of fitting parameters and $<\tau>$ for CL-OH

Temperature (°C)	τ (s)^{a}	β (-)^{a}	$<\tau>$ (s)
130	125250	0.76	147800
140	52510	0.69	67400
150	20648	0.72	25600
160	8463	0.68	11100

a) see the explanation of the fitting parameters in the main text.

15. Relaxation data for the sample with a smaller fraction of tertiary amines

To investigate the effects of tertiary amine fraction, we prepared another terpolymer containing a smaller fraction of DMAEA by varying the initial feed mole ratio. Concretely, the mole ratio of BA: DMAEA: ECHMA was set to 6.5: 0.5: 1, where the fraction of DMAEA was half of that in P-N. The synthesis was confirmed by ^{1}H-NMR (Figure S13) and SEC (Figure S14). The M_n and $Đ$ was 24 k and 1.3. This terpolymer (coded as P-N-0.5) was cross-linked by the reaction with the disulfide cross-linker, 2,2'-dithiodibenzoic acid, and the obtained sample is coded as CL-N-0.5. The plateau modulus of CL-N-0.5 was similar to these of CL-N and CL-OH (Figure S15), and thus the cross-link density was identical.

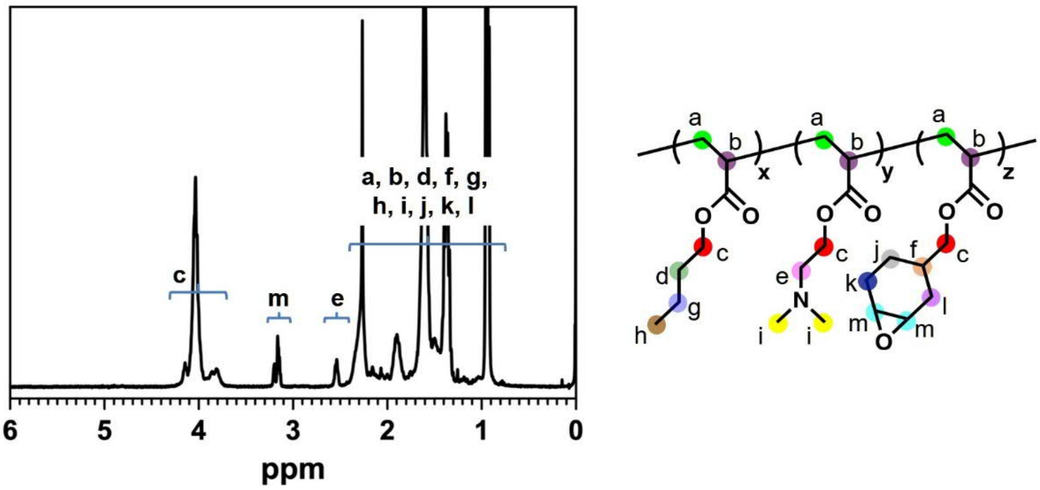

Figure S13. ^{1}H-NMR spectrum of P-N-0.5 in $CDCl_3$.

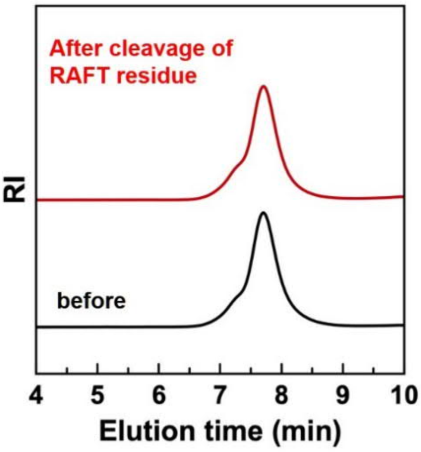

Figure S14. SEC curves for P-N-0.5 before and after cleavage of the end RAFT residue.

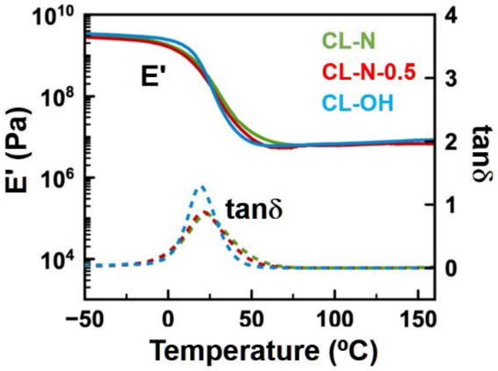

Figure S15. Temperature-sweep rheology data for CL-N-0.5, where the data of CL-N and CL-OH are shown for comparison.

The stress relaxation data of CL-N-0.5 was then compared with CL-N and CL-OH (Figure S16a). Plots of $<\tau>$ was shown in Figure S16b, where $<\tau>$ was estimated based on the fitting analysis (see the explanation in the main text). The results indicate the relaxation rate of CL-N-0.5 was indeed middle between CL-N and CL-OH. In addition, the E_a value (~85 kJ/mol) was also located in the middle.

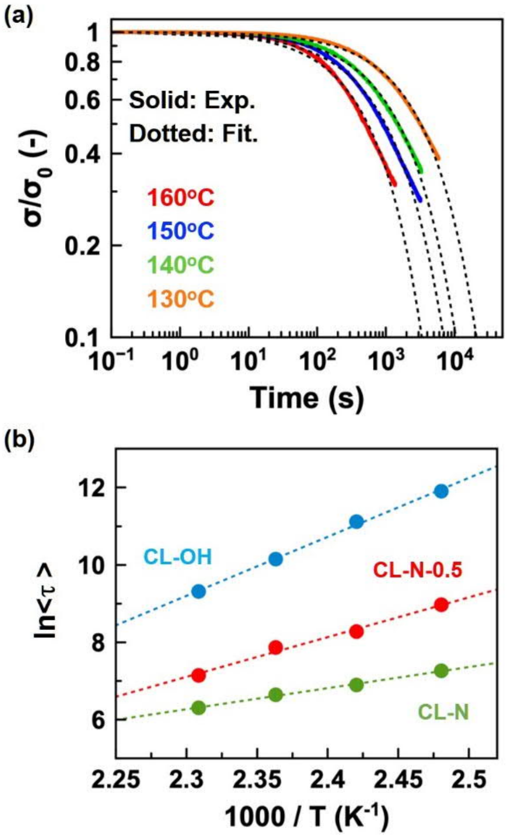

Figure S16. (a) Stress relaxation curves for CL-N-0.5. In the Y-axis, the stress (σ) was normalized by the initial stress (σ_0). The dotted curves indicate the fitting curves based on the KWW function (see main text). (b) Temperature dependence of $<\tau>$ for CL-N, CL-OH, and CL-N-0.5. The dotted line indicates the approximate straight line between the points.

Table S3. Summary of fitting parameters and $<\tau>$ for CL-N-0.5

Temperature (ºC)	τ (s)[a]	β (-)[a]	$<\tau>$ (s)
130	5685	0.64	7810
140	2754	0.63	3930
150	1787	0.61	2610
160	946	0.66	1270

a) see the explanation of the fitting parameters in the main text.

16. ESR spectra at 120 ºC

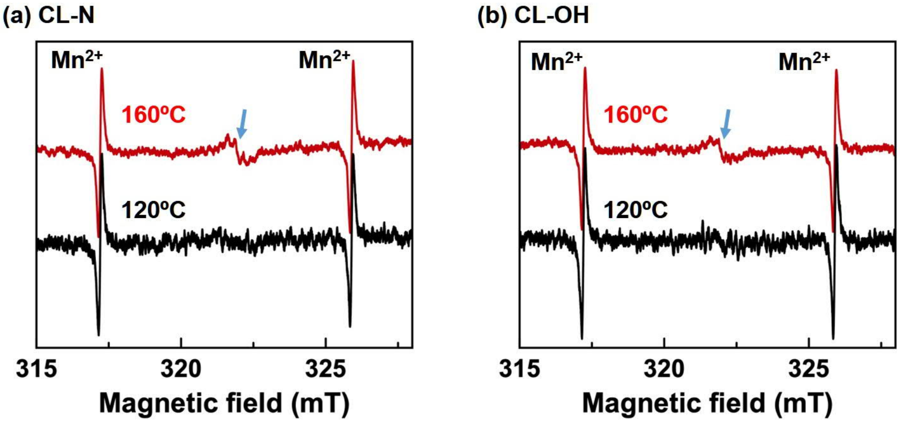

Figure S17. ESR spectra measured at 120 and 160 ºC for CL-N and CL-OH. The arrows represent the signal from sulfide radical, and the distinct outside signals were from Mn^{2+} used for the magnetic field calibration.